

Hierarchical Disk Galaxy Assembly as the Origin of Scatter in the $z \sim 1$ Stellar Mass Tully-Fisher Relation

Nicola Atkinson¹, Christopher J. Conselice^{1*}, Nicole Fox¹

¹ *University of Nottingham, School of Physics & Astronomy, Nottingham, NG7 2RD UK*

Accepted ; Received ; in original form

ABSTRACT

Recent observations of distant disk galaxies show that there is little to no evolution in the relation between maximum rotation speed and stellar mass at $z < 1.2$. There is however a significant scatter between these two quantities whose origin is uncertain. We show in this paper that this scatter is at least partially the result of galaxy merging, revealing that disk galaxy growth at $z < 1$ is fundamentally hierarchical. We carry this out by calculating CAS (concentration, asymmetry, clumpiness) structural parameters using archival Hubble Space Telescope imaging of 91 high-redshift disk galaxies at $0.4 < z < 1.0$ with robustly measured stellar masses and rotational maximum velocities taken from Conselice et al. (2005). We separate our sample into two redshift bins divided at $z = 0.7$, and investigate deviations from the stellar-mass Tully-Fisher relation in both the M_* and V_{\max} directions, and how these correlate with structural asymmetries. We find a significant ($> 3\sigma$) correlation between the residuals from the stellar-mass Tully-Fisher relation in both the M_* and V_{\max} directions, and high asymmetries. This result holds after we remove contributions from star formation and edge-on galaxies which can produce higher asymmetries unrelated to merging. While there are a few cases in which our disk galaxies have very large asymmetries, and are potentially involved in major mergers, in general these asymmetries are smaller than the major merger limit. It is therefore likely that these galaxies are forming hierarchically through minor galaxy mergers, which is also suggested by the constant slope and zero point of the stellar mass Tully-Fisher relation during the same epoch.

Key words: Galaxies: Evolution, Formation, Structure, Morphology, Classification

1 INTRODUCTION

In the standard cosmological model the mass density of the universe is dominated by collisionless dark matter. Structure within the universe forms as a result of small density fluctuations, which induce gravitational clustering. In this picture, smaller objects collapse and undergo mergers to form larger objects. Dark matter halos, in which galaxies are believed to be embedded, form in this way. These halos form gravitational potential wells, which collect gas necessary for star formation, creating a visible galaxy (e.g., Lacey & Cole 1994).

Much observational work has been carried out to aid our understanding of the history of mass assembly in galaxies to test these ideas. Whilst dark matter halos build up through hierarchical methods, governed primarily by density fluctuations in the early universe, the assembly of stellar content

is far more complex. It is clear that gaseous dissipation, the mechanics of star formation, and the feedback of stellar energetic output of the baryonic material of galaxies must all be considered in understanding stellar mass build-up, along with the assembly of galaxies through merging and accretion of existing stellar systems.

There are two popular ideas for explaining how the bulk of stars in galaxies are put into place, namely the monolithic collapse, and the hierarchical model. Both of these models predict how disk galaxies and ellipticals form. In the monolithic collapse scenario stars are concentrated into a bulge due to a rapid collapse of either gas, or existing stars, contained by its dark matter halo. This bulge can then acquire a disk by cooling of gas from the intergalactic medium (IGM) onto the spheroid, with star formation occurring as the gas clouds collide (Steinmetz & Navarro 2002; Abadi et al. 2004). In this model, different galaxy morphologies form due to discrete differences in environment, and the amount of matter present. In the hierarchical model, spiral bulges are

* E-mail: conselice@nottingham.ac.uk

a result of the merging of existing stellar and gaseous systems. These mergers lose angular momentum through the ejection of material leading to high stellar concentrations in the central regions, comprising of both existing stars and those formed out of the colliding gas.

Whilst there is evidence for massive galaxies forming hierarchically from mergers, creating elliptical galaxies and bulges, the formation process for disk galaxies remains largely unknown. One way to test this is through the Tully-Fisher relation between a galaxy's luminosity and its maximum rotational velocity (V_{\max}), as well as the evolution of this relationship, and its internal scatter. A more fundamental stellar mass Tully-Fisher (SMTF) relation also exists, whereby a galaxy's luminosity is substituted by its stellar mass (M_*). Bell & De Jong (2001) and Verheijen (2001) both found a tight correlation between maximum rotational velocity and stellar mass, and K-band luminosity, for disk galaxies in the local universe.

To search for evolution in the SMTF relation Conselice et al. (2005a) examined the SMTF relation at $0.2 < z < 1.2$ with respect to the $z \sim 0$ relation (Bell & de Jong 2001). Conselice et al. (2005a) found that the relationship between stellar mass and V_{\max} does not evolve significantly up to $z \sim 1.2$. Since stellar mass in disks at $z < 1$ must be increasing due to observed star formation, the conclusion from this work is that disk galaxy formation at $z < 1.2$ is hierarchical - gas is accreted along with dark matter in a manner which preserves the stellar mass TF relation. There is also no evolution in the stellar mass-total halo mass relation at the same redshifts (Conselice et al. 2005a), suggesting that the stellar and dark mass components of disk galaxies grow simultaneously throughout this period. This result was later also found to be the case by e.g., Flores et al. (2006) and Bohm & Ziegler (2006).

Another feature of the stellar mass-TF relation at high redshift is that there is a significant scatter from the best fit relation. The origin of this scatter is a major question that has been addressed in several previous works (e.g., Kannappan, Fabricant & Franx 2002; Kassin et al. 2007). The origin of the scatter in the TF relation can be the result of different mass to light ratios, different formation histories in terms of star formation and mass assembly, or intrinsic to disks themselves. By examining the stellar mass Tully-Fisher we are removing the mass to light ratio differences and thus can test whether the scatter is due to formation histories and/or is intrinsic, or otherwise due to observational errors. For high-redshift galaxies Kassin et al. (2007) examined the internal kinematics of $z < 1.2$ galaxies with a range of galaxy morphologies, and found that the TF relation is highly morphologically dependent. Non-disturbed spirals form a clear ridge-line in the TFR that follows the local relation. Almost all major mergers, disturbed, and compact galaxies have lower rotational velocities compared to the $z \sim 0$ values, producing a large scatter. A larger scatter in the TF relation is also found for galaxies in close pairs with kinematic disorders (Barton et al 2001), and for irregular galaxies (Kannapan et al. 2002).

Recently, Flores et al. (2006) related the deviations from the TF relation with kinematic properties of galaxies using Integral Field Unit (IFU) observations. All rotating pure disks, with regular rotation curves, were found to lie along the $z \sim 0$ line. The majority of galaxies with perturbed kinematics

were found within the 3σ scatter quoted by Conselice et al (2005a), and galaxies with very complex kinematics deviated the most. These galaxies deviate from the stellar mass TF relation due to too high or low rotational velocities, at a given stellar mass, produced by disturbed kinematics. If these eventually form well ordered disk galaxies and move onto the $z \sim 0$ line, this evolution may result from their stars and gas settling into more circular orbits, hence increasing, or decreasing the measured V_{\max} .

Conselice et al. (2005a) also found that many disk galaxies deviate strongly from the relation between stellar mass and maximum rotational velocity. One hypothesis proposed in Conselice et al. (2005a) and tested in this paper is that these galaxies are undergoing accretion of intergalactic matter, or satellite galaxies, which increases both the baryonic and stellar mass at roughly the same rate. We test this hypothesis in this paper through an analysis of the CAS parameters for a sample of 91 disk galaxies used in the Conselice et al. (2005a) study. If disks are forming hierarchically from stellar+gaseous mergers then the systems which deviate the most from the stellar mass TF relation should display signatures of recent merging or accretion activity in their CAS parameters.

This paper is organised as follows. In §2 we present our sample of galaxies, the data we use to perform this analysis, and the techniques used to derive evolution. §3 presents the results of our analysis, §4 is a discussion of our results, and §5 is a summary of our findings. Throughout this paper we use the standard cosmology of $H_0 = 70 \text{ km s}^{-1} \text{ Mpc}^{-1}$, and $\Omega_m = 1 - \Omega_\lambda = 0.3$, and a Chabrier IMF for our stellar masses measurements, unless otherwise noted.

2 SAMPLE AND METHODS

2.1 Data and Sample

The sample used in this analysis is taken from Conselice et al. (2005a), and initially consisted of 101 disk galaxies imaged with the Hubble Space Telescope (HST) with rotation curves measured from the Keck Telescope, and for which we have deep near-infrared imaging. These disks were selected to have inclinations $> 30^\circ$ in order to remove nearly face-on systems so that rotation curves could be measured. However, no upper limit was set to the inclination, thus it is possible that dust lanes in edge-on galaxies are present. Our sample covers the redshift range $0.2 < z < 1.2$, enabling any evolution in structural parameters to be seen over half the age of the universe. For the purpose of image analysis, all galaxies were chosen to have no obvious interacting companions, or obscuring foreground stars.

High resolution images of these galaxies were taken from two sources, archival HST Advanced Camera for Surveys (ACS), and HST Wide Field Planetary Camera 2 (WFPC2) imaging. After removing systems that we could not use, the total galaxy sample used in this project consisted of 91 disk galaxies. The redshift range was also reduced to $0 < z < 1$ to avoid strong morphological k-corrections that can result in ambiguous results (e.g., Taylor-Mager et al. 2007).

The ACS Wide-Field Channel (WFC) allows deep, wide-field survey capabilities from the visible to NIR wavelengths. This difference however, should not pose a problem

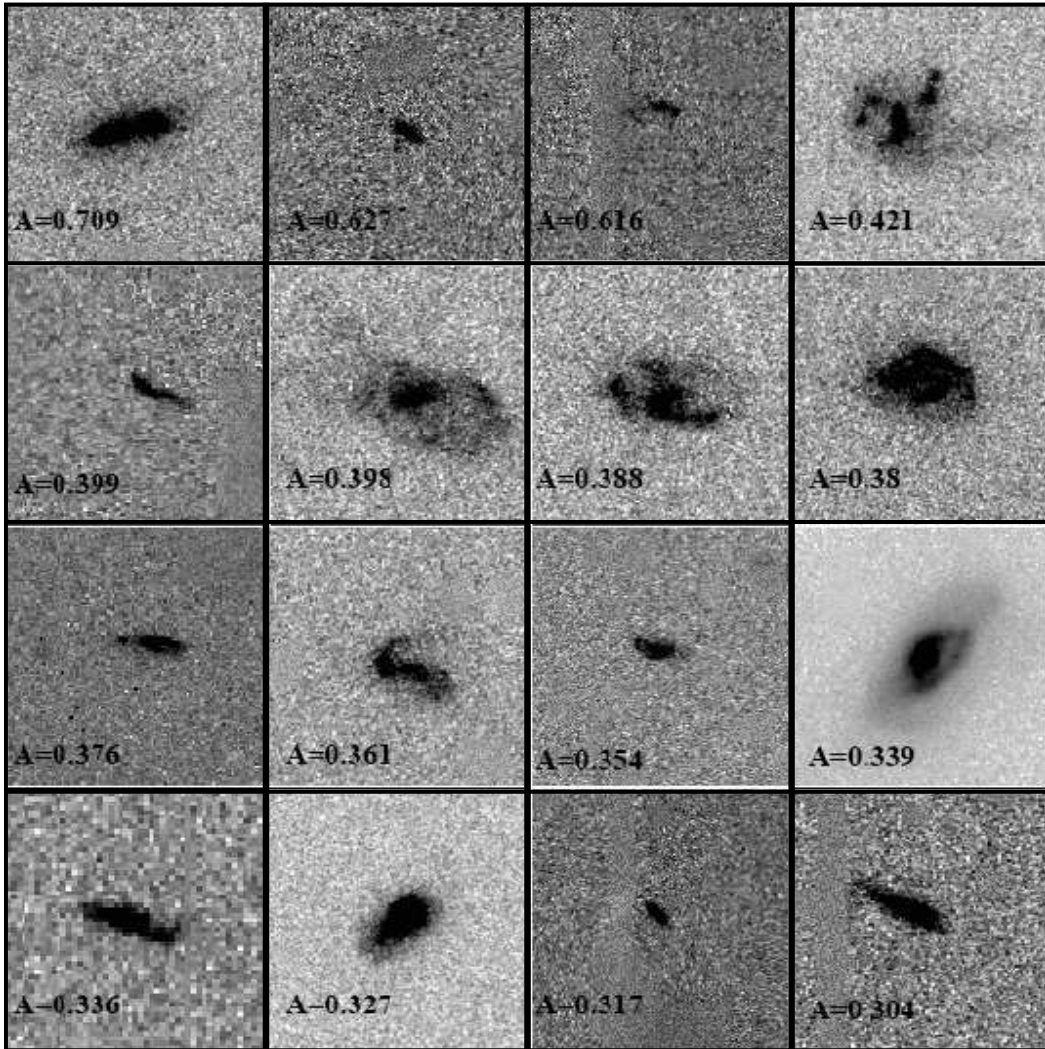


Figure 1. Galaxies with high asymmetries, $A > 0.3$. The asymmetry (A) is indicated in the bottom left of each image. This Hubble Space Telescope imaging is taken with the ACS and WFPC2 camera in the F814W band.

when determining CAS parameters for these galaxies, since the C and A indices are sensitive to bulk structures, and are therefore remarkably stable with respect to resolution (Conselice 2003). The clumpiness parameter is more sensitive to resolution, and thus has a larger uncertainty in the WFPC2 images. The ACS WFC has a FOV of $202''$ and an optimal resolution of approximately $0.049''/\text{pixel}$. The WFPC2 images comprise data from four cameras, the Wide-Field cameras (WF2, WF3, WF4), and the planetary camera (PC). The WF2, WF3 and WF4 have optics that are essentially the same, each having an FOV corresponding to a resolution of $0.0996''/\text{pixel}$.

A total of 52 of the galaxies within our sample are found in HST images taken by the ACS Wide-Field Camera (WFC) in the Groth Strip area of the DEEP survey (Vogt et al. 2008, in prep). The remainder of the images are taken from archival WFPC2 programs including imaging of the Hubble Deep Field-North and the Canadian-France Redshift Survey (CFRS). These images were available with

their corresponding segmentation and weight maps, needed for determining the CAS parameters of a galaxy (e.g., Conselice et al. 2007c, in prep). The images we use are taken within the F814W (I-band) filter and the F606W (V-band) filter.

2.2 Galaxy Rotation Curves

The estimated disk galaxy V_{max} values used in the project were obtained by Vogt et al (1996, 1997, 2008) and Conselice et al. (2005a) using moderate-resolution spectroscopy from the Keck 10-m ground-based telescope with the LRIS instrument (Oke et al. 1995). Spatially resolved spectra of these disk galaxies at $0.2 < z < 1.2$ were fit with a single (or double) Gaussian profile to each emission line (or doublet), most commonly the [OII] doublet, and the [OIII] and $H\beta$ lines (Vogt et al. 1993). The position, amplitude, and width of the lines were found from best-fits to single or double Gaussian profiles, and the S/N ratio was calculated within

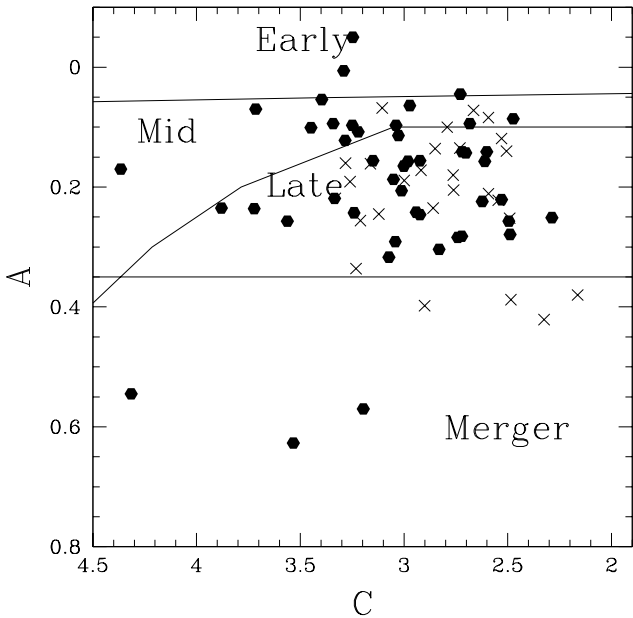


Figure 2. The concentration-asymmetry diagram for our sample of disk galaxies in the observed F814W-band. Solid symbols are for galaxies at $z < 0.7$ and crosses are for those at $z > 0.7$. As can be seen, the vast majority of our sample of disks are found within the region of CAS space occupied by late-type or early-type disk galaxies. There are however clearly some examples of disk galaxies which appear to have very high asymmetries.

these limits. The central wavelengths of these profiles were used to construct velocity rotation curves, where the Gaussian fit met minimum requirements in height and width of 5σ and 3σ , respectively. However, the typical value was 10σ for both amplitude and width (Vogt et al. 1996).

Determining the rotation curves for high redshift galaxies cannot be as accurately done as for local galaxies. The sizes of the disk galaxies within our sample are typically just slightly larger than the size of the seeing, and the width of the spectroscopic slit. Therefore, wavelength shifts in the observed emission lines from which we measure V_{\max} represents a combination of the spatial distribution in the disk’s velocity and the emission line surface brightness. To correct for this Vogt et al. and Conselice et al. (2005a) adopted a simple exponential model for each galaxy, matching inclination and orientation relative to the slit from measurements from HST images. The rotational velocities from such models are assumed to have a linear form, rising out to a maximum at 1.5 times the disk scale length, R_d , and then remaining flat at V_{\max} . The seeing was taken into account by convolving the model with an appropriate Gaussian, and the model emission lines were fit identically to the spectral data. Iterative adjustments were made to the rotational velocity of each galaxy model until the simulated and observed emission lines matched.

Factors such as a misalignment of the slit with the galaxy major axis, and varying inclination are also considered when performing this simulation, as these also contribute to errors in the estimation of V_{\max} . It was also necessary to consider the relatively large uncertainty in the

scale length (R_d) when estimating V_{\max} . Conselice et al. (2005a) measured the disk scale-length, R_d , by fitting a two-component model to the surface brightness distribution of each galaxy. However, they found that the errors in R_d resulting from this method may be underestimated. An additional uncertainty from the fitted R_d values must therefore also be considered. In total, the derived measurement of V_{\max} is inferred with an associated uncertainty of 20%-30% (Conselice et al. 2005a).

Whilst the above method works adequately for a well formed disk with circular orbits throughout, if a galaxy is undergoing a major or minor merger, the V_{\max} estimate could be either higher or lower than expected for non-merging disks. In the beginning stages of a merger, the rotational motion of the two component galaxies may remain intact. However, at higher redshift, the components may not be spatially resolved. Only the spectra from the outer most parts of this combined system are considered when fitting the simple exponential profile, hence increasing the estimation of V_{\max} . Conversely, in the central stages of a merger, rotational velocity could be largely destroyed, hence lowering the V_{\max} estimate. Consequently, both positive and negative deviations in V_{\max} from the $z \sim 0$ TFR could indicate mergers (see §3.2.1).

2.3 Stellar Masses

The stellar masses used within our sample are the same as those calculated by Conselice et al. (2005a). These stellar masses were determined using standard methods explained in e.g., Brinchmann & Ellis (2000), Bundy et al. (2005, 2006) and Conselice et al. (2007a). This method for calculating stellar mass combines near-infrared (NIR) luminosities and optical photometry of galaxies with well-known redshifts to estimate stellar masses based on fitting the observed SED to different star formation models. We utilise models from Bruzual & Charlot (2003) with a Chabrier IMF to compute our stellar masses (see also Conselice et al. 2007). Unlike other methods of determining stellar mass of galaxies, this has no bias against galaxy type or orientation. The bands we used in Conselice et al. (2005a) to calculate the stellar masses are the K-band ($2.2\mu\text{m}$), and the optical bands as observed with the Hubble Space Telescope.

2.4 CAS Parameters

We utilise the CAS (concentration, asymmetry, clumpiness) parameters (Conselice et al. 2000a,b; Bershady et al. 2000; Conselice 2003) to determine the morphological and structural state of our disk galaxy sample. CAS parameters provide classifications in terms of the concentration of light (C), asymmetry (A), and the clumpiness (S). Each of these parameters, and the apparent total magnitudes, are defined within the Petrosian radius aperture of,

$$R_{\text{Petr}} = 1.5 \times r(\eta = 0.2),$$

where the dimensionless parameter η , is an intensity ratio of the enclosed light as a function of radius (e.g., Bershady et al. 2000). More than 99% of the light is contained within this radius for most galaxy profiles, and the light within

the radius is the closest estimate to the true total magnitude, assuming a perfect Gaussian light profile (Bershady et al. 2000). This radius is dependent only on the surface brightness within a given radius, and no assumptions are made about the shape of the galaxy’s light profile. Below we briefly describe the CAS parameters and how they are calculated within this radius.

2.4.1 Concentration

The concentration index (C) is a measure of a galaxy’s integrated light distribution and is defined by Bershady et al. (2000) and Conselice (2003) as,

$$C = 5 \times \log \left(\frac{r_{80}}{r_{20}} \right), \quad (1)$$

where r_{80} and r_{20} are the radii inside which 80% and 20% of the light is contained, respectively. The concentration of light correlates with the bulge to total light flux ratio of galaxies, and their masses (Conselice 2003). Thus concentration relates to a galaxy’s formation history in a broad sense. For disk galaxies, concentration is found between $2.5 < C < 4$, and galaxies with low central surface brightness generally have the lowest light concentrations. This also corresponds to those galaxies with low internal velocity distributions on average (e.g., Bershady et al. 2000; Conselice 2003).

2.4.2 Asymmetry

Conselice et al. (2000a,b) and Conselice (2003) define the asymmetry index (A) by rotating a galaxy image by 180° about its centre, and subtracting the flux values at each pixel from those of its pre-rotated image, I_0 . The intensities of the absolute value of the residuals of this subtraction are then summed over all pixels, and are compared with the total galaxy flux. The basic mathematical definition of the asymmetry is,

$$A = \min \left(\frac{\sum |I_0 - I_{180}|}{\sum |I_0|} \right) - \min \left(\frac{\sum |B_0 - B_{180}|}{\sum |B_0|} \right), \quad (2)$$

where the B -component is a correction for the background noise. Slightly negative A values may be caused by the background correction if the galaxy is non-disturbed and compact with small residual values. Asymmetry is sensitive to any feature which produces distorted light distributions. These include galaxy interactions/mergers, and dust lanes occurring in edge-on disk galaxies (Conselice et al. 2000a). Star formation causes small scale disturbances, seen as high frequency information in an image, which will also produce asymmetries.

Star formation however does not cause as high of an asymmetry signal comparable to the other dynamically induced features. The asymmetry can also be affected slightly by the effects of projecting a 3-D galaxy onto a 2-D image, especially at very high inclinations (Conselice et al. 2000). A high asymmetry, by itself, therefore cannot be used to uniquely identify a merger.

N-body models of active ongoing galaxy mergers also show that systems that have recently undergone a merger, or those at the beginning or end, of a major merger, may not appear highly asymmetric. For this reason the asymmetry

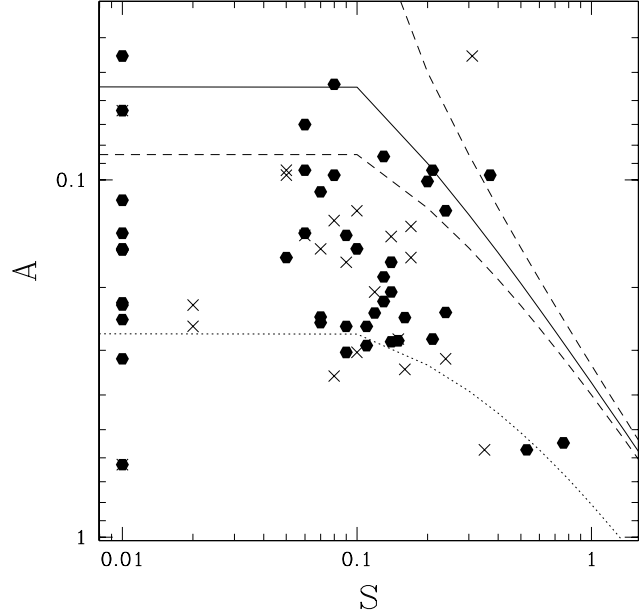


Figure 3. The clumpiness-asymmetry diagram for our sample of disk galaxies in the observed F814W-band. The solid points are for $z < 0.7$ galaxies and the crosses are for those at $z > 0.7$. The solid line on this diagram shows the location of nearby normal galaxies as found at $z \sim 0$, with the 3σ scatter from this relationship shown as the dashed lines. The dotted line shows the derived relation for systems which deviate strongly from the relation between A and S . The large number of points at $S = 0.01$ are for those galaxies which are too small to have a correctly measured S parameter (Conselice 2003).

index is not sensitive to all phases of merging, and Conselice (2003, 2006) show that in a given sample the total number of galaxies undergoing major mergers would be underestimated by roughly a factor of ~ 2 if only using the asymmetry parameter. However, no non-mergers have extremely high asymmetries unless they are at high inclinations, where dust lanes and projection effects become important.

2.4.3 Clumpiness

The clumpiness parameter (S) is a measure of the patchiness of a galaxy’s light distribution. It is defined by Conselice (2003) as the ratio of the amount of light contained in high frequency structure (within the defined galaxy aperture) to the total amount of light in the galaxy. In order to compute this quantity, the original galaxy image is smoothed by a filter of width σ to reduce its effective resolution, thus removing all high frequency information. This smoothed image is then subtracted from the original image to obtain a residual image leaving only the high frequency components. This flux is then summed over all pixels and a background brightness value is subtracted. Mathematically, clumpiness (S) values are obtained through the formula,

$$S = 10 \times \left[\left(\frac{\sum (I_{x,y} - I_{x,y}^\sigma)}{\sum I_{x,y}} \right) - \left(\frac{\sum (B_{x,y} - B_{x,y}^\sigma)}{\sum I_{x,y}} \right) \right], \quad (3)$$

with any negative differences forced to zero. The inner parts of each galaxy are also not considered in the computation of

S since they often contain high frequency information unrelated to stellar light distributions (Conselice 2003). Since disturbances due to star formation appear as high frequency information, a large amount of star formation results in high S values. High clumpiness is therefore more prominent in star forming galaxies, while $S \sim 0$ for ellipticals which contain little star formation and appear smooth.

2.4.4 CAS Computations and Meaning

Before performing our structural parameter measurements foreground stars, background galaxies, cosmic rays, hot pixels, and light gradients are removed from the images. Some of these features are removed by the SExtractor segmentation maps, while those missed by this process are cleaned by hand. Many of the galaxies in our sample are also found in more than one HST archival image. We use the image with the highest signal to noise, and the lowest amount of contamination from other light sources, and those in which the galaxy is not close to the edge of the CCD chip.

As we use both I-band (F814W) and V-band (F555W) images in our analysis, we can compare directly how the CAS values change between these two wavelengths. We find that the C , A and S parameters in the V-band were larger by roughly 3%, 9% and 109%, respectively, compared to the I-band values. However, the C parameters for the V-band are only higher than the I-band images for 66% of the images. Similarly, for the A and S parameters the V-band images have parameters higher than the I-band images for 58% and 76% of the images, respectively.

We apply the CAS structural parameters to decipher any structural evolution from low to high- z in our disk galaxy sample, and to determine how this correlates with the scatter from the SMTF relation. It is therefore important to consider how measurements of these parameters change as galaxies become less resolved and fainter due to cosmological effects. To address this, Conselice (2003) simulated nearby galaxies at various higher redshifts to determine the effects of redshift on measuring galaxy structures. Conselice (2003) find that the asymmetry and clumpiness indices decline, on average, as a function of redshift, and the concentration increases slightly. The amount of this change using 1-orbit HST images is roughly $\delta A = -0.03$, $\delta S = -0.25$, and $\delta C = 0.1$ at $z \sim 1$.

In addition to the CAS measurements we also visually classified all galaxies, and found disks that appear to be disturbed or compact, and compared these to the calculated parameters. The most disturbed, highly asymmetric galaxies are shown in Figure 1. We find that galaxies with high A values in general look by eye more disturbed. All galaxies with low asymmetries appear as symmetric, and sometimes compact, disks.

More than 80% of the galaxies with $A > 0.3$ are found within the ACS images, with three WFPC2 images in this group. The larger percentage of ACS images with high asymmetry values suggests that the image resolution affects the calculation of this parameter. However, calculation of the asymmetry parameter is mostly dependent on large scale-structures, which are not easily lost through reduced resolution. Therefore it is possible that there could simply be few high asymmetry galaxies in the WFPC2 sample and upon in-

spection, there were none in which a galaxy appeared highly asymmetric in its large scale structure.

Conversely, all galaxies with $A < 0.05$ were found in the WFPC2 images. We find that 45% of the WFPC2 images have zero clumpiness values in both bands, compared to only 4% in the ACS images. The S parameter is dependent on high frequency information, which is lost in low resolution imaging. For the lower resolution WFPC2 images, the galaxy subtends fewer pixels and, combined with the use of only the central region for computation, there is a very limited amount of information available from which to deduce meaningful clumpiness values.

In several cases a galaxy could not be measured within the CAS system, and was excluded from the sample, since it was too contaminated by light from a neighbouring source. Often this contamination was the result of nearby sources that could not be completely removed successfully. Consequently, CAS parameters are calculated for a total of 91 disk galaxies.

2.4.5 Identifying Morphological Peculiarities

Asymmetry and clumpiness parameters reveal active evolution in the form of interactions/mergers and star formation, respectively. We thus use the CAS parameters to determine how galaxy formation processes correlate with deviations from the SMTF relation. Given the postulate that galaxies in our sample are deviating from the SMTF relation due to mergers, we would expect that galaxies which deviate highly will contain higher asymmetries. Before we can test this, we must examine the methods used to determine the presence of galaxies undergoing active merging.

As described in Conselice et al. (2000a,b) and Conselice (2003), a selection of $A > 0.35$ for nearby galaxies will give a nearly clean selection of active ongoing major mergers, uncontaminated by normal galaxies. Another way to identify mergers, or galaxies strongly interacting, is to examine the relationship between the A and S parameters. Conselice (2003) found a relation for non-merging galaxies from all morphologies, given by,

$$A = (0.35 \pm 0.03) \times S + (0.02 \pm 0.01). \quad (4)$$

Deviations from this fit, due to increased asymmetries, are caused by distortions in a galaxy's stellar light distributions, possibly indicating mergers. This is certainly the case for nearby galaxies in rest-frame optical light (Conselice 2003). However, since systems that have recently finished a merger, or are at the beginning of a merger, will have settled in their distribution, these deviations will not locate all ongoing mergers (Conselice 2006). Galaxies involved in minor mergers should also deviate slightly from the A-S relation compared with non-mergers, since their asymmetries should also be higher than average (Conselice 2006).

3 RESULTS

3.1 CAS Volume

The CAS parameters for our sample of galaxies are compared to the CAS volume classification in Figures 2 & 3. Since our sample was chosen to only contain disk galaxies,

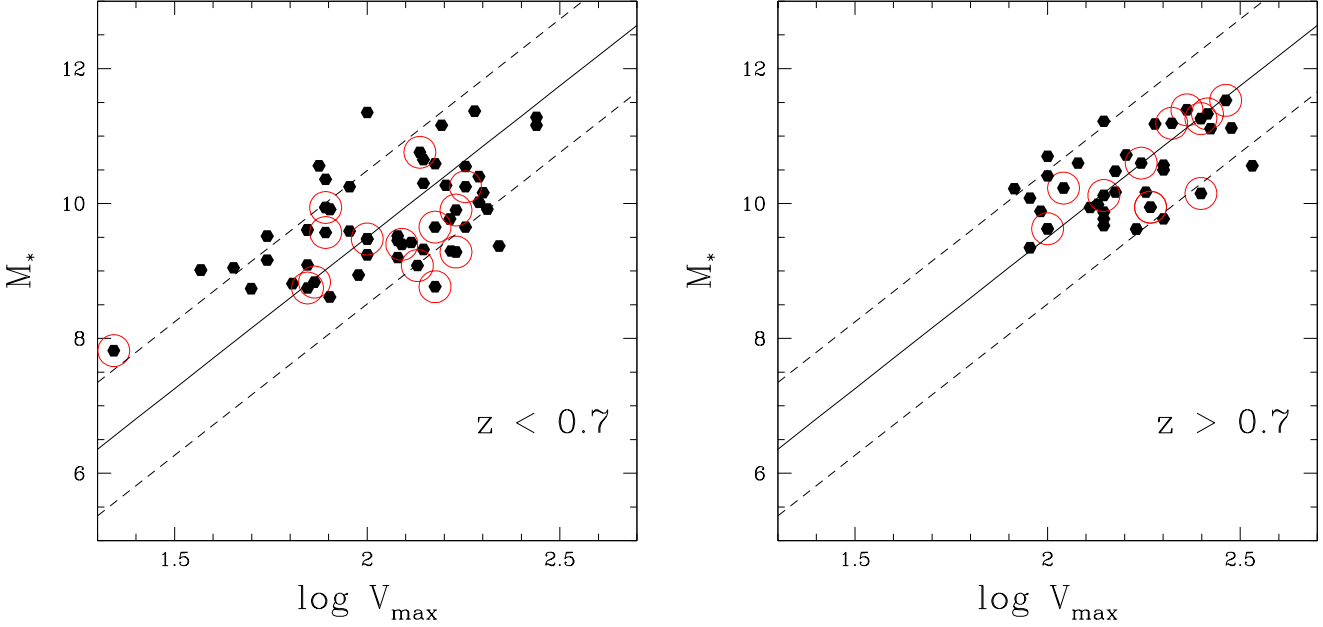


Figure 4. The Tully-Fisher relation for galaxies within our sample at $z < 0.7$. The solid line shows the $z \sim 0$ relation given in Conselice et al. (2005a), and the dashed-lines show the 3σ scatter in this relationship. The error-bars for these points are discussed in detail in Conselice et al. (2005a). M_* is measured in solar mass units (M_\odot), and V_{\max} is measured in km s^{-1} . The right hand side shows the TF relation for galaxies within our sample at $z > 0.7$. Galaxies which are circled on this diagram are for those which have asymmetry values $A > 0.25$.

we expected that our galaxies would lie within the bounds of the CAS disk morphologies: early-type disks, late-type disks, and edge-on disks. This implies that the majority of the calculated parameters would lie within the region $2.7 < C < 4.3$, $0.03 < A < 0.28$, and $0 < S < 0.65$, with the 1σ variation in the classification system taken into account (Conselice 2003).

We find that 70% of the disks in our sample have parameters which placed them within the CAS region enclosing disks and spiral galaxies. The average redshift is $z = 0.49$ for those galaxies classified as late-type disks within CAS, and $z = 0.68$ for early-type disks, suggesting that these could be correctly identified, as more massive disks are selected at the higher redshifts (Conselice et al. 2005a). We further find that 18% of our sample have asymmetries $A > 0.3$, and the values correlate by eye to the amount of disk distortion, as seen in Figure 1.

We compare the asymmetry index (A) with the clumpiness index (S) for the $z < 0.7$ and $z > 0.7$ redshift bins in Figure 3. If we utilise the relationship for non-mergers we can infer if any galaxies outside the 3σ scatter could be mergers. However, due to resolution and signal to noise effects, the A-S relation is offset with respect to the $z \sim 0$ relation due to a lowered resolution and signal to noise, and we have to consider this offset when using the A-S diagram.

The A-S relation for non-mergers in Figure 3 is plotted as the solid line. After accounting for redshift corrections, we find that $\sim 50\%$ of our galaxies lie outside of the 3σ scatter. We exclude any galaxies which lie within the 3σ scatter of the relationship for non-merging galaxies, and plot a best fit line for the remaining points, weighted by the parameter

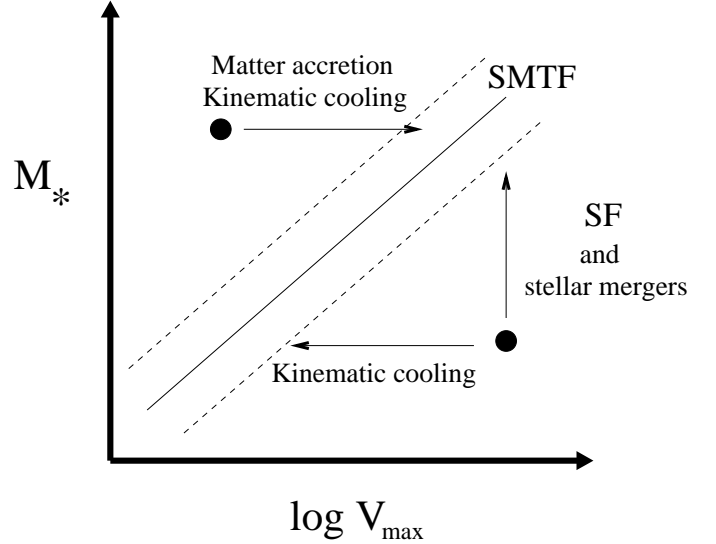


Figure 5. Graphical representation for how galaxies which deviate from the SMTF relation can evolve onto it. Shown by lines with arrows are the direction in this plot a galaxy would evolve due to kinematic cooling after a merging event which can both lower and increase the value of V_{\max} . Also shown are how with new star formation (SF), and stellar mass accretion events, the value of M_* can increase over time.

errors, to calculate the relation between S and A for merging galaxies. For the the WFPC2 images, this was fit as,

$$A = (0.7 \pm 0.2) \times S + (0.23 \pm 0.03), \quad (5)$$

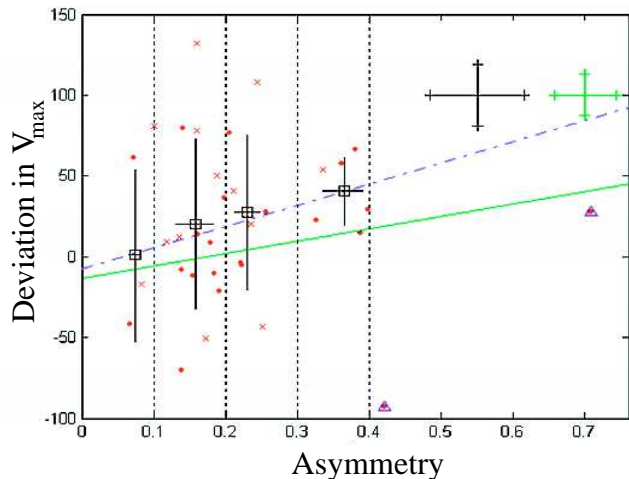


Figure 6. The A parameter calculated from galaxies in both ACS and WFPC2 I-band images (F814W) plotted with the deviation in V_{\max} from the $z \sim 0$ relation. The small solid points are for galaxies from the ACS imaging, which the crosses are for the WFPC2. Galaxies above the $z \sim 0$ line in Figure 4 have positive residuals and those below have negative. The solid green line shows a best fit with no exclusion of points. The blue dashed line shows the best fit, where the high asymmetry points indicated by blue triangles have been excluded. Black squares indicate the average values of all points contained within each A -bin marked by the dotted black lines. Black crosses mark the corresponding standard deviations in the scatter for each group of points. Black and green error-bars indicate ACS and WFPC2 errors respectively.

where the errors quoted are the 95% confidence bounds. Using the ACS images, the merging relation is very similar,

$$A = (0.6 \pm 0.3) \times S + (0.21 \pm 0.03), \quad (6)$$

as shown in Figure 3. Both of the above fits (Eq 5 & Eq 6) have a RMSE of 0.09, showing good relations. The overlap in the error-bounds of the above relations indicate that the wavelength and instrument dependency in the CAS parameters must alter the A and S parameters in a systematic way.

A larger number of merging galaxies are expected at higher redshift (e.g., Conselice et al. 2003). Since merging systems have higher A values, we examine the correlation between redshift and the asymmetry index. This was done by examining the relationship between asymmetry and redshift for only galaxies with calculated asymmetries $A > 0.25$. Based on this, we find that there are a greater number of highly asymmetric galaxies at higher redshift. There are very few galaxies with $A > 0.25$ at redshift $z < 0.4$. We also investigate how the concentration parameter varies as a function of redshift, finding no significant correlation.

3.2 Structure-Tully-Fisher Relation at $z < 1.2$

3.2.1 Motivation

As we have described in the introduction and in §2.2, correlating the deviations from the SMTF with galaxy structure may reveal the origin of the large scatter in SMTF relation at $z < 1$. Before we analyse how the scatter in the SMTF

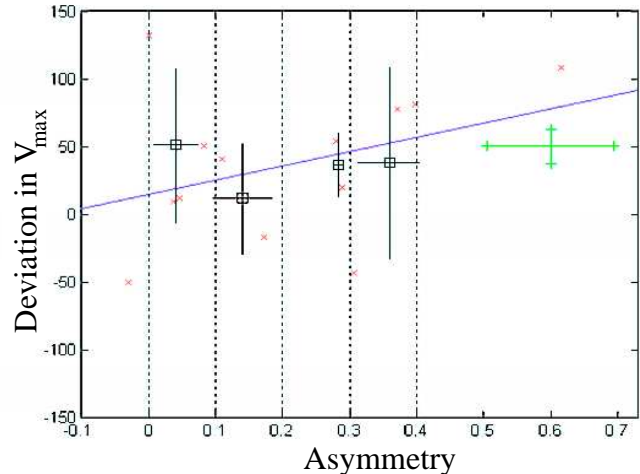


Figure 7. The asymmetry parameter calculated from V-band WFPC2 images plotted against the deviation in V_{\max} from the $z \sim 0$ relation. Galaxies above the $z \sim 0$ line in Figure 4 have positive residuals and those below have negative residuals. The solid blue line shows the best fit. The black squares indicate the average values as described in Figure 6. Errors are also as described in the Figure 6 caption.

relates to galaxy structure, it is important to understand the motivation behind this test. Figure 4 shows the SMTF relation as observed at $z < 1$, which was previously published in Conselice et al. (2005a). As can be seen, there is significant scatter in the relation between V_{\max} and M_* , although there is a clear general relationship between these two quantities.

Figure 5 gives a graphical model for how galaxies which do not fall along the SMTF can evolve onto it over time. The processes by which a galaxy can move onto the SMTF relation include kinematic cooling from a past galaxy merger, as well as an increase of stellar mass from star formation, and through the accretion of existing satellite galaxies. Whether these processes can occur depends on if a galaxy is located above the SMTF relation or below it. If a galaxy is located above the relation, then the only way it can reach the relation is through the growth of dark matter without accompanied star formation, and/or the kinematic cooling of a galaxy after it undergoes a dynamical event with another galaxy, either through a merger or an interaction of some type.

For those galaxies below the relation, the evolution onto the SMTF can occur either through stellar mass evolution through star formation, or accretion of satellite galaxies, and/or through kinematic cooling after a merging or interaction event. In all but one case, the evolution onto the SMTF relation involves hierarchical growth. We can rule out interactions with other galaxies that do not involve merging, as our disk galaxy sample do not have any nearby companions. Therefore, any evolution on the SMTF relation in the V_{\max} direction involves either kinematic cooling from a merger, or the accretion of matter from the intragalactic medium. Evolution onto the SMTF from galaxies above the relation therefore must involve some type of dynamical accretion or merging event.

On the other hand, it is possible that galaxies below

the SMTF reach the relation over time through star formation. The other possibility is that the scatter in the SMTF relation at these redshifts is purely due to observational errors. By correlating this scatter with galaxy structure, and determining the significance of any trends, we can make this distinction.

3.2.2 The Stellar Mass Tully-Fisher

To examine how structure correlates with the scatter in the stellar mass TF relation, we split our galaxy sample into two redshift bins, $z < 0.7$ and $z > 0.7$. We determine deviations from the SMTF based on the best fit to the observed SMTF relation using our own data, and to the $z \sim 0$ relation. The zero point of the Bell & de Jong (2001) $z \sim 0$ SMTF relation was fit such that the standard deviation from the line was at a minimum. For the $z < 0.7$ systems this was found to be:

$$\log M_* = (4.49 \times \log V_{\max}) + 0.37, \quad (7)$$

and for $z > 0.7$ the relation we fit is,

$$\log M_* = (4.49 \times \log V_{\max}) + 0.29. \quad (8)$$

These derived relations are both within the error bounds of the local relation found by both Conselice et al (2005a), and Bell & de Jong (2001). This is consistent with no large scale evolution of the SMTF relation over the redshift range $0 < z < 1$. Hence, we will assume that our best fits in Eq 7 & 8 describe the SMTF relations at their respective redshifts. If we utilise either the $z \sim 0$ relation, or these internal fits, we find very similar results in what follows.

Galaxies which deviate by more than 3σ from the SMTF relation were visually inspected for disturbances, and the CAS parameters analysed for any trends. Over redshifts $0 < z < 1$, we found that deviating galaxies covered a large range of asymmetry values, $0 < A < 0.62$. We also checked if any deviating galaxies appear as either face-on or edge-on disk galaxy systems. Face-on galaxies could have inaccurate V_{\max} estimates, and dust lanes may affect the asymmetries of edge-on galaxies. When looking at images of deviating galaxies, only one galaxy appears face-on, displaying a central bar structure.

Deviations in terms of V_{\max} and M_* from the best fit $z \sim 0$ relations (Eq 7 & Eq 8) were calculated in each of our two redshift bins. Deviations are such that if the value is higher than predicted by the SMTF relation, then the residual is negative. These deviations were compared with the asymmetry and clumpiness parameters. First, we found no clear and obvious relation between highly deviating galaxies and the asymmetry parameter for galaxies at $z < 0.7$. However, Figure 6 and Figure 7 show the relation between V_{\max} deviations from the SMTF relation, and the asymmetries of these galaxies at $z > 0.7$, where we do see a significant correlation within the I-band and V-band images, respectively.

We fit a line to the V_{\max} residuals, as a function of asymmetry, weighted by the errors in the deviation in V_{\max} . This fit is shown in Figure 6 as a solid green line. However, a better fit was obtained if the two high A galaxies, indicated with blue triangles, were excluded. The standard deviations in the scatter place the points on this new relation, which is shown as a blue dashed line. For galaxies in the V-band imaging, a weighted best-fit line was derived, shown as the

solid green line in Figure 7. Although no points have been excluded, this relation is less reliable since there are only 13 V-band galaxy images at $z > 0.7$. However, a positive correlation is seen in both Figure 6 and Figure 7.

We utilise Monte Carlo simulations to test the validity of these correlations, and to compare whether this increase in asymmetry with SMTF residuals is significant given the large uncertainties in measuring M_* and V_{\max} . To carry out this Monte Carlo simulation we place each data point randomly along its V_{\max} error-bar. This simulation was repeated 100,000 times, and we find that the significance of the correlations are 3σ and 1σ , for the I-band and V-band deviations from the $z \sim 0$ line, respectively. The actual significance of these correlations is likely even higher than this, as these errors likely have a normal distribution.

As explained in §2.2, both positive and negative deviations in V_{\max} could indicate mergers. Therefore, we also studied the equivalent of Figure 6 and Figure 7 for the absolute residuals in V_{\max} from the $z \sim 0$ line. No significant trend (1σ) was seen in this data, showing that not all highly deviating galaxies have high A values. It also shows that on average galaxies with a higher asymmetry have a larger positive deviation in V_{\max} from the best fit SMTF relation.

3.2.3 Contribution from Star Formation

Since a high asymmetry index can be produced through both mergers/interactions and star formation, we investigate whether the correlation between the asymmetry and deviations from V_{\max} are produced by star formation. To investigate this, a new parameter $A' = A - S$ is computed for all galaxies in our sample. This new parameter indicates in a sense ‘true’ asymmetries, with the contribution from star formation and dust removed by the clumpiness parameter which correlates with small-scale features in a galaxy (Conselice 2003). The relation between A' and the SMTF relation residuals is shown in Figure 8. We find no major change to the trend seen in Figure 6 between the asymmetry itself and the SMTF relation residuals, suggesting that this correlation is produced through large-scale features in a galaxy. The two galaxies with high asymmetries in Figure 6 also have high S parameters, and their positions have moved significantly, and they no longer deviate strongly from the trend. The original asymmetry values for these galaxies are thus clearly affected by star formation, but the vast major of asymmetries are not.

Whilst deviations in V_{\max} from the $z \sim 0$ TFR are useful for identifying galaxies which may have undergone kinematic changes, deviations in M_* may indicate either star formation or stellar mass accretion (§3.2.1). Galaxies which have large positive deviations in M_* resulting from a merger would be expected to have high asymmetry values. Such a relation can be seen in Figure 8.

In general, galaxies that display a higher positive deviation in the SMTF relation residuals in M_* space have higher computed asymmetries. Monte Carlo simulations of this correlation shows that this result is significant at $> 3 \sigma$. However, an exception to this is one galaxy which has a high positive deviation in M_* , despite its relatively low asymmetry ($A = 0.16$). The asymmetry parameters measured from the V-band images showed a similar trend to that seen in

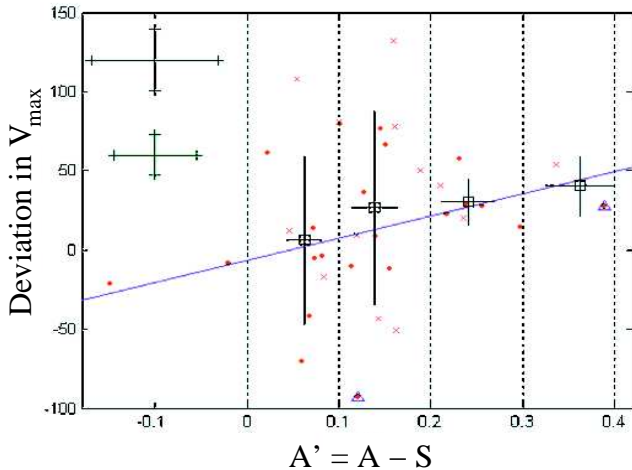


Figure 8. The $A' = A - S$ parameter calculated from the I-band images compared with the deviation in V_{\max} from the $z \sim 0$ relation. Blue triangles denote the two high asymmetry galaxies shown in Figure 6. The solid blue line shows a best fit. The error in A' is from the combined errors in the A and S parameters. All other features are as outlined in Figure 6.

Figure 9, but due to the small sample size cannot be used to infer any significant relation.

Since mergers often induce star formation, we examine the relationship between clumpiness and the deviations in both V_{\max} and M_* . However, no trend was seen at any redshift, partially due to the difficulty of measuring the clumpiness parameter.

4 DISCUSSION

We find in this paper that the deviations from the SMTF relation in both the M_* and V_{\max} directions correlate with galaxies with higher internal asymmetries. We have also found that disk galaxies at higher redshifts display on average higher asymmetries.

The number of mergers seen in our sample, based on the asymmetry parameter, falls short by a factor of ~ 2 of the 22% of mergers found occurring in disks at $z \sim 0.6$ by Flores et al (2006). This is consistent with the postulate in Conselice (2003) that in a sample of galaxies, the total number undergoing mergers would be underestimated by a factor of two when considering analysis of the asymmetry parameter alone. Since Flores et al (2006) used IFU measurements to look at perturbed galaxy kinematics their estimate of the number of mergers is thought to be more accurate than CAS parameters allow. However, our sample is three times larger than Flores et al. (2006) and covers a wider range of redshifts.

The derived SMTF relation for our sample, at both $z > 0.7$ and $z < 0.7$, are similar to each other, and are consistent with no significant evolution of the SMTF relation over the redshift range $0 < z < 1$ (Conselice et al. 2005a). The origin of these deviations from the SMTF may arise from accreted gas, stars, and dark matter from the IGM in

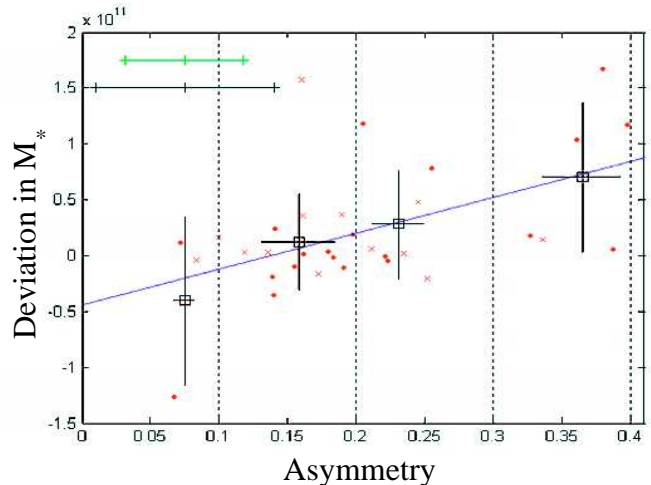


Figure 9. The asymmetry parameter calculated from the I-band images compared with the deviation in M_* from the $z \sim 0$ relation. Galaxies above the $z \sim 0$ line in Figure 4 have positive residuals and those below have negative residuals. The solid blue line shows a best fit. The black squares indicate the average values of all the points contained within each A-bin marked by the dotted black lines. The black crosses mark the corresponding standard deviations in the scatter for each group of points. The green and black error-bars indicate the WFPC2 and ACS errors, respectively.

the form of minor mergers or smooth accretion. These accretion mechanisms can increase the stellar mass with either pre-formed stars, or by inducing star formation. Since mass cannot be lost from a galaxy, evolution in this case must settle towards higher V_{\max} . This settling could be caused by circularisation of gas orbits or gaseous dissipation to the disk plane, ending with the growth of a gaseous disk.

Deviations below the $z \sim 0$ SMTF relation are for disks with either a lower M_* and/or a higher V_{\max} than expected. If these deviations are due to the early stages of a merger, the increased V_{\max} may result from individual components not being resolved in the ground based spectra. This causes incorrect V_{\max} estimations, and a falsely decreased stellar to halo mass ratio. The deviation could also be caused by a disk galaxy which has not yet formed all its stellar components and the inferred stellar to halo mass ratio could be evolving. Galaxies found below the $z \sim 0$ line therefore would need to evolve in stellar mass through accretion processes or star formation, so that this ratio would become that expected for the disk galaxy TF relation. This reasoning suggests that the majority of scenarios for deviations both above and below the $z \sim 0$ line can be explained by the occurrence of mergers.

At $z > 0.7$, we find that $\sim 70\%$ of disks with stellar masses $M_* > 10^{10} M_\odot$ scatter to low V_{\max} , which shows a slight increase compared with those at $z < 0.7$. For $M_* < 10^{10} M_\odot$ galaxies at $z > 0.7$ there are no systems which deviate from the $z \sim 0$ line by more than 3σ , likely an effect of the sampling bias. Lower mass disks may have been missed at high redshift because they often are not bright enough to observe rotation curves. At lower redshift however, there are large deviations at both high and low V_{\max} . This suggests that lower mass galaxies at low redshift may be still forming.

Interestingly, we do not find a significant trend between asymmetries and residuals from the SMTF relation

for galaxies at $z < 0.7$. A possible reason for this is that structural relaxation is quicker than the internal velocity relaxation after a merger. In such a case, the stellar structures are relaxed before V_{\max} , which would be the case as the V_{\max} values originate from larger radii where the time-scale needed for dark matter in the halo to settle are longer than the stars at the centre of the disk.

Figure 6 shows that there is a positive deviation in V_{\max} from the SMTF relation at higher A . This means that highly asymmetric galaxies have large scatter at lower V_{\max} values. This supports the idea that these deviations are due to the central stages of mergers. In this case the galaxy appears asymmetric, and has a random velocity distribution causing the lower V_{\max} measurement.

It is also apparent that deviations at higher V_{\max} (negative residuals) most often have low asymmetry values. This could be explained if the galaxy is at the beginning stage of a merger where its asymmetry parameter has not yet been affected. An exception to this observation however, is one galaxy which has a large deviation at higher V_{\max} , but a relatively high asymmetry of $A = 0.42$. We suggest that this galaxy fits within our hypothesis that deviations at higher V_{\max} indicate the beginning stages of a merger. However, in this case the merging components can be visually seen, producing a high asymmetry despite the structure of the individual components remaining intact.

When examining deviations from the best-fit SMTF relation in M_* , we find that, in general, larger deviations of higher M_* corresponded to higher A values (Figure 9). This can be explained if the galaxy has had mass accreted from the IGM or a merger, disrupting its structural appearance but with V_{\max} not yet settled. There are no positive deviations in M_* larger than $\sim 10^{11} M_{\odot}$, which is approximately 80% of the stellar mass of the Milky Way. This is consistent with the idea that minor mergers are the cause of the deviations. Figure 9 also shows that deviations at lower M_* correspond to lower A values. This could be explained if these galaxies have not fully evolve to their final stellar mass.

5 SUMMARY

We present in this paper a structural analysis of 91 disk galaxies within the redshift range $0 < z < 1$ to determine if the scatter in the stellar mass Tully-Fisher (SMTF) relation at $z < 1$ is produced through mergers or accretion. Previous analysis of the kinematic (V_{\max}) and stellar mass (M_*) properties of these galaxies show no significant evolution in the zero point or scatter of the SMTF relation out to $z \sim 1$ (Conselice et al. 2005a). There is however a significant amount of scatter in the SMTF relation whose origin is unknown.

We investigate whether deviations from the stellar mass Tully-Fisher relation, as seen by Conselice et al (2005a), can be explained by the presence of morphologically disturbed galaxies whose CAS structural parameters are measured. We find that on average galaxies which deviate the most from the stellar mass Tully-Fisher relation are asymmetric systems. This correlation is significant at $\sim 3 \sigma$, and is not produced by star formation or edge-on galaxies. We interpret this to imply that disk galaxies at $z < 1$ are forming hierarchically either through accretion of satellite galaxies,

or intergalactic baryons and dark matter. This is furthermore seen through how deviations occur from the stellar mass Tully-Fisher relation, as $\sim 70\%$ of our disks at $z > 0.7$ deviate above the $z \sim 0$ relation. Growth onto the stellar mass Tully-Fisher relation can in this case only occur through kinematic cooling to raise the value of V_{\max} , or through the addition of matter, without significant star formation, through accretion or merging. We see a significant positive correlation between both V_{\max} and M_* deviations with asymmetry, suggesting that both could be evolving simultaneously.

Our statistical analysis also suggests that more disk galaxies with $A > 0.25$ are present at high redshift. Both of these results support the hierarchical model for disk galaxy formation at $z < 1$, even after the major epoch of merging has ended and the major properties of disks are in place (Conselice et al. 2003; Jogee et al. 2004; Conselice et al. 2005b; Ravindranath et al. 2006). Within our galaxy sample, we furthermore find that 70% of the most asymmetric galaxies are at $z > 0.4$, implying strong dynamical evolution in the last 5 Gyrs. This is further supported when observing the scale of deviations in stellar mass, which are typically that of a low-mass galaxy. Our primary conclusion is that while disk galaxies are morphologically present in abundance at $z < 1$, these systems are still forming hierarchically during this time due to collisions with existing galaxies, or discrete baryonic/dark matter dominated clouds.

There are a number of improvements which could enhance our understanding of this problem. This is necessary since both CAS parameters, and the method of estimating V_{\max} and M_* , have their limitations. Few low stellar mass galaxies are present in our sample due to the original selection criteria, and the fact that more distant low mass galaxies are harder to measure rotation curves for. We therefore do not have a completely representative sample of disk galaxies over the redshift range $0 < z < 1$. For galaxies within our sample, V_{\max} may also have been miss-estimated due to observational errors in the ground-based slit spectroscopy. The method we use is not sufficient to imply detailed interior kinematics of a galaxy. However, combined with knowledge of their luminosity, it is sufficient to recognise those that do not have well formed disks. In conclusion, we find that positive and negative deviations from the $z \sim 0$ TF relation seen by Conselice et al (2005a) are indicative of disturbed galaxies. Whilst this is a step towards understanding the origin of the TF relation, detailed IFU spectra are needed to confirm this, and to determine exactly what mechanism causes this disruption.

We thank Nicole Vogt for useful advice and the University of Nottingham for their support.

REFERENCES

- Abadi, M.G., Navarro, J.F., Steinmetz, M., Eke, V.R. 2003, *ApJ*, 597, 21
- Bell, E.F., De Jong, R.S. 2001, *ApJ*, 550, 212
- Bershady, M.A., Jangren, J.A., Conselice, C.J. 2000, *AJ*, 119, 2645
- Bohm, A., Ziegler, B.L. 2006, *astro-ph/0601505*
- Brinchmann, J., Ellis, R.S. 2000, *ApJ*, 536, 77L
- Bruzual, G., Charlot, S. 2003, *MNRAS*, 344, 1000

- Bundy, K., et al. 2006, ApJ, 651, 120
 Bundy, K., Ellis, R.S., Conselice, C.J. 2005, ApJ, 625, 621
 Conselice, C.J., Bershad, M.A., Jangren, A. 2000a, ApJ, 529, 886
 Conselice, C.J., Bershad, M.A., Gallagher, J.S. 2000b, A&A, 354, 21L
 Conselice, C.J. 2003, ApJS, 147, 1
 Conselice, C.J., Bershad, M.A., Dickinson, M., Papovich, C. 2003, AJ, 126, 1183
 Conselice, C.J., Bundy, K., Ellis, R., Brichmann, J., Vogt, N., Phillips, A. 2005a, ApJ, 628, 160
 Conselice, C.J., Blackburne, J., Papovich, C. 2005b, ApJ, 620, 564
 Conselice, C.J. 2006, ApJ, 638, 686
 Conselice, C.J., et al. 2007, ApJ, 660, 55L
 Flores, H., Hammer, F., Puech, M., Amram, P., Balkowski, C. 2006, A&A, 455, 107
 Jogee, S., et al. 2004, ApJ, 615, 105L
 Kassin, S.A., et al. ApJ, 660, 35L
 Lacey, C., Cole, S. 1994, MNRAS, 271, 676
 Ravindranath, S., et al. 2004, ApJ, 604, 9L
 Steinmetz, M., & Navarro, J.F. 2002, New Astronomy, 7, 155
 Taylor-Mager, V., Conselice, C., Windhorst, R., Jansen, R. 2007, ApJ, 659, 162
 Verheijen, M.A.W. 2001, ApJ, 563, 694
 Vogt, N.P., Forbes, D.A., Phillips, A.C., Gronwall, C., Faber, S. M., Illingworth, G.D., Koo, D.C. 1996, ApJ, 465, 15
 Vogt, N.P., et al. 1997, ApJ, 479, 121L